Jour. of the KGS Vol. 16, No. 3, June 2000, pp 131~144

Parametric Study on the Impact-Echo Method using Mock-Up Shafts

모형말뚝을 이용한 충격반향기법의 영향 요소 연구

Kim, Dong-Soo [*1] 김 동 수
Kim, Hyung-Woo [*2] 김 형 우

요 지

본 연구는 비검측공 시험법으로서 널리 사용되고 있는 충격반향기법(impact-echo test)의 적용성을 수치해석 및 실내 실험을 통하여 분석해 보았다. 즉, 결함이 없는 말뚝과 결함이 있는 말뚝에 대하여 1차원 및 2차원 축대칭 유한요소해석을 실시하였으며, 또한 모노캐스트라고 하는 일종의 플라스틱 원형 봉의 말뚝에 축대칭 공극, 비축대칭 공극, 병목부 및 단면 확대부와 같은 결함을 각각 크기와 깊이를 변화시켜 제작한 후 공기 중과 지반 내부에서 충격반향기법 실험을 수행하였다.

실험 결과 충격반향기법의 말뚝 결함 탐지능력은 수치해석에서 얻은 결과와 함께 결함의 크기와 위치에 영향을 받는 것으로 나타났으며 결함의 크기가 커질수록 탐지의 정확도가 향상되는 것을 알 수 있었다. 결함의 상대면적이 말뚝 단면적의 50% 이상이면 충격반향기법에 의하여 결함의 위치를 파악할 수 있는 것으로 나타났으며, 공기 중 보다 지반에 근입된 말뚝의 경우가 더욱 명확한 신호를 제공해주는 것으로 나타났다. 그리고 시간영역의 신호가 주파수 영역의 신호 보다 말뚝의 결함 크기에 더 민감히 반응하므로 주파수 영역에서 탐지할 수 없는 작은 크기의 결함을 시간 영역에서는 탐지할 수 있는 것으로 나타났다.

Abstract

In this study, the non-borehole seismic impact-echo method was employed to evaluate the integrity of drilled shafts, and parametric simulations of impact-echo method were carried out numerically and experimentally. One- and two-dimensional finite element studies of mock-up shafts that were made of monocast material were performed for both solid shafts and shafts containing defects such as axisymmetric voids, non-axisymmetric voids, necks and bulbs. And subsequently experimental studies were carried out to verify the finite element models using same mock-up shafts. These experimental studies were carried out for shafts embedded in soil as well as in the air. It was shown that the results of experimental studies were in good agreement with the those of numerical studies, and the accuracy of the impact-echo method was influenced by the type, size and location of the defects. And it was also revealed that the axisymmetric void, non-axisymmetric void and necks could be detected if the area reduction were about 50% or greater. Moreover, the impact-echo responses for the shafts containing various defects were obtained in both time and frequency domains, and the better possibilities of detecting the flaws in the time domain were also investigated.

Keywords : Impact-echo test, Nondestructive tests, Drilled shafts, Stress wave propagation, Defects, Finite element, Parametric study

*1 Member, Associate Professor, Dept. of Civil Engrg., KAIST
*2 Member, Graduate Student, Dept. of Civil Engrg., KAIST

1. Introduction

Recently the drilled shafts are being frequently used for deep foundations of large-scale structures in Korea, and therefore it becomes more and more important to detect the defects such as voids, cracks, necks, bulbs, soil intrusions, and soft bottom(Kim and Park, 1999). Since the defects in the drilled shafts may cause a serious decrease of the support load and an increase of settlement, the development of integrity testing technologies is essential.

In practice, impact-echo testing, impulse response testing, cross hole sonic logging testing (CSL), and gamma-gamma testing methods are commonly in use to evaluate the integrity of the drilled shafts. The CSL and gamma-gamma testing methods require the boreholes that guide the source and receiver, whereas impact-echo testing and impulse response testing methods do not require them. Therefore, the additional cost of borehole installation makes the CSL and gamma-gamma testing methods expensive. However, CSL can detect multiple defects and locate them accurately, and also have no depth limitation. In contrast to those borehole seismic methods, the impact-echo testing and impulse response testing methods are cheap to perform, and can be performed on any shaft provided that access can be gained to the shaft head. Currently CSL is being used in the field of quality control of drilled shafts, but the method is so expensive that it is not economical to extend the CSL to all of the drilled shafts. Therefore the non-borehole seismic methods such as impact-echo testing and impulse response testing are to be used as assistant, and thus, the reliable non-borehole seismic methods should be developed essentially. Accordingly, the integrity evaluation and quality control of drilled shaft can be accomplished thoroughly with both borehole and non-borehole seismic methods.

In this study, as a cost-effective and easily applicable test, impact-echo method is introduced to evaluate the integrity of drilled shafts. The method was initially developed by the National Institute of Standards and Technologies in USA, and has been more improved by Sansalone and her co-workers (Sansalone, and Streett, 1997 ; Lin et al., 1991). However, it seems that the acquired signals of the impact-echo are subjective to interpret, and therefore the integrity evaluation of the shaft is dependent upon the engineer. Thus, it is required that the integrity evaluation by impact-echo method should be both objective and quantitative.

So, the feasibilities of the method were reviewed by using both the extensive numerical and experimental studies. The one- and two-dimensional axisymmetric finite element studies were performed using ABAQUS program for the mock-up shafts including axisymmetric voids, non-axi-symmetric voids, necks, and bulbs as well as solid shaft. Subsequently, the experimental studies were carried out to verify the numerical results using the same mock-up shafts embedded in soil as well as in the air. Finally, the limitations as well as feasibilities of impact-echo method are identified.

2. Numerical Studies

2.1 General

In the three-dimensional dynamic problem for an elastically isotropic material, (u, v, w) are considered to be displacements corresponding to a chosen cartesian coordinate system. And it is assumed that the material has mass density ρ, Young' modulus E, Poissons's ratio υ, and Lame constants λ and G, where $\lambda+2G$ is the constrained modulus and G is the shear modulus. The general equations of motion in the absence of body forces are given by

$$(\lambda+G)\frac{\partial e}{\partial x}+G\nabla^2 u-\rho\frac{\partial^2 u}{\partial t^2}=0$$

$$(\lambda+G)\frac{\partial e}{\partial y}+G\nabla^2 v-\rho\frac{\partial^2 v}{\partial t^2}=0 \qquad (1)$$

$$(\lambda+G)\frac{\partial e}{\partial z}+G\nabla^2 w-\rho\frac{\partial^2 w}{\partial t^2}=0$$

where e is the volumetric strain and $\nabla^2=\partial^2/\partial x^2+\partial^2/\partial y^2+\partial^2/\partial z^2$ is the three-dimensional Laplacian operator (Timoshenko et al. 1970). In equation (1), there are two

kinds of stress waves propagating inside the material : (a) transverse wave, (b) longitudinal wave.

The transverse wave involves no volume change and all particles are moving perpendicular to the direction of wave propagation. If the x-axis is taken in the direction of propagation, it can be shown that for transverse waves, u = v = 0 and v is a function of x only. Then,

$$G\frac{\partial^2 v}{\partial x^2} - \rho\frac{\partial^2 v}{\partial t^2} = 0 \qquad (2)$$

or

$$\frac{\partial^2 v}{\partial t^2} = V_s^2 \frac{\partial^2 v}{\partial x^2} \qquad (3)$$

where,

$$V_s = \sqrt{\frac{G}{\rho}} = \sqrt{\frac{E}{2(1+\upsilon)\rho}}$$

And for longitudinal waves, v = w = 0 and u is a function of x only. This results in a single equation of motion as follows,

$$(\lambda + 2G)\frac{\partial^2 u}{\partial x^2} - \rho\frac{\partial^2 u}{\partial t^2} = 0 \qquad (4)$$

or

$$\frac{\partial^2 u}{\partial t^2} = V_p^2 \frac{\partial^2 u}{\partial x^2} \qquad (5)$$

where,

$$V_p = \sqrt{\frac{(\lambda + 2G)}{\rho}} = \sqrt{\frac{E(1-\upsilon)}{(1+\upsilon)(1-2\upsilon)\rho}}$$

If the plane cross sections assumed to be unchanged and only axial stresses are present, and the stresses are uniformly distributed over the cross section, the longitudinal motions for a bar are controlled by one-dimensional equation.

$$\frac{\partial^2 u}{\partial t^2} = V_{rod}^2 \frac{\partial^2 u}{\partial x^2} \qquad (6)$$

where, $V_{rod} = \sqrt{\frac{E}{\rho}}$ is "rod wave speed".

From equation (6), it follows that the longitudinal wave propagates in this rod with a velocity Vrod, which is constant and depends only on the material properties E and ρ. Any function u(x, t) that will satisfy the above equation (6) is as following,

$$u(x,t) = f(x - ct) = A \sin\frac{2\pi}{\lambda}(x - ct) \qquad (7)$$

where, A is an arbitrary constant. Equation (7) represents a sinusoidal wave with wave length λ, period λ/V_{rod} and wave propagation velocity V_{rod}. The axial stress is then given by

$$\sigma_x = E\varepsilon_x = E\frac{\partial u}{\partial x}$$

or

$$\sigma_x = \frac{E}{V_{rod}}\frac{\partial u}{\partial t} = \rho V_{rod}\frac{\partial u}{\partial t} \qquad (8)$$

Since any pulse can be described by means of a Fourier analysis in terms of its sinusoidal components, and each component propagates at the same velocity V_{rod}, no phase differences develop at remote stations along the rod, and hence no distortion of the pulse shape results (Abramson et al., 1958).

2.2 Dynamic Modeling

The mock-up shafts considered in this paper were discretized using truss elements in the one-dimensional analyses and four node axisymmetric elements in the two-dimensional analyses. The diameter and the length of the shaft is 0.1m and 1.0m respectively. The modulus of elasticity, Poisson's ratio, and the density were 4.17 GPa, 0.45, and 1152 kg/m³, respectively, and these constants resulted in rod wave speed of 1880 m/sec.

In the finite element modeling of the shaft, the duration of the impact (t_c) is an important factor because it determines the frequency content of the stress wave that is generated(Sansalone and Streett, 1997). Nearly all the energy (about 98%) is contained in frequencies less than about $2.5/t_c$.

Sansalone (1997) suggested that the duration of the impact (t_c) should be carefully determined by the diameter (D) and the drop height of the steel sphere, and it could be approximated by

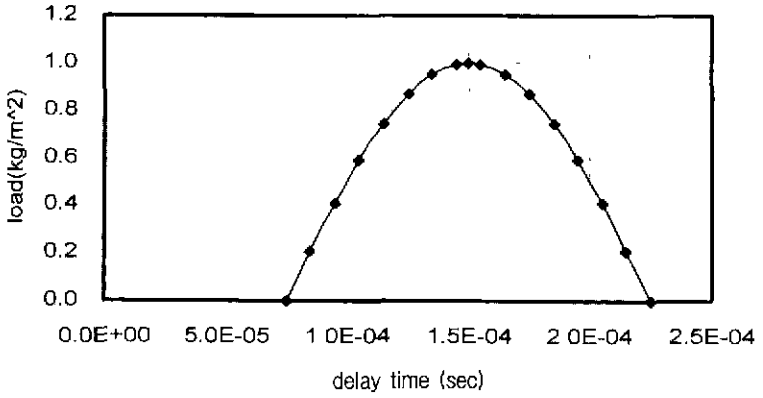

Fig. 1 Sinusoidal impact of half a cycle duration

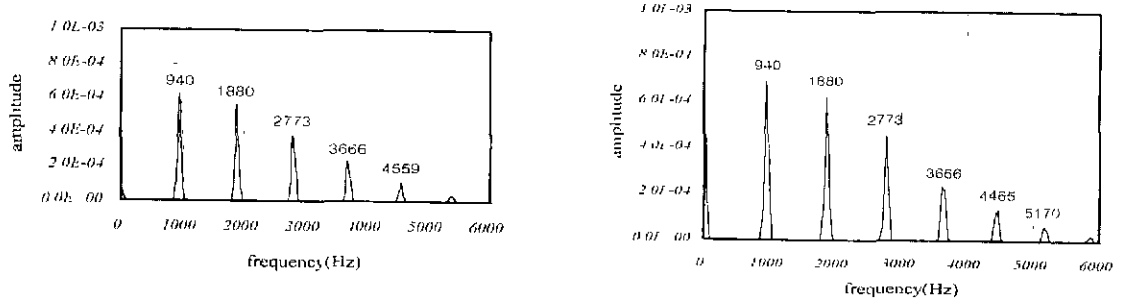

(a) One-dimensional model (b) Two-dimensional axisymmetric model

Fig. 2 Amplitude spectrums of solid shaft in the air

$$t_c = \frac{0.0043\ D}{h^{0.1}} \tag{9}$$

where, t_c is in seconds and D and h are in meters.

In this finite element study, the duration of the impact was determined to be 1.5×10^{-4} sec to generate the frequency contents up to 17 kHz, and the loading pressure was assumed to have a sinusoidal impact of half a cycle as shown in Fig. 1.

Another important factor influencing the results of finite element analysis is the element size, and it is shown that in order to obtain a satisfactory result, the element size should be less than about one tenth the wavelength of the highest frequency waves propagating in the structures.

$$\triangle l = \frac{\lambda}{10} \tag{10}$$

For a rod wave speed in monocast mock-up shaft of about 1880 m/sec, nearly all the wavelengths in the propagating waves would be longer than 1880 t_c/2.5. Thus, the maximum element size must be less than 188 t_c/2.5 to model wave propagation problems accurately, so the element size was determined to be 1cm.

2.3 Numerical Studies for the Solid Shafts in the Air

To simulate the monocast mock-up shaft in the air, the surrounding air was modeled as a weak and light material with minimal acoustic impedance. Therefore, the shear wave velocity, Poissons ratio, and the density were assumed to be 0.05m/sec, 0.01, and 0.001kg/㎥ respectively. Fig. 2 shows the amplitude spectrums determined by one-dimensional and two-dimensional axisymmetric finite element model. The resonance peaks occur at 940, 1880, and 2773 Hz which are exactly same in each model, and these peak frequencies are identical with those determined by following equation (11).

$$f_n = \frac{n\ V_{rod}}{2T} = n \cdot \frac{1880m/\sec}{2\times1.0m} = 940Hz,\ 1880Hz,\ 2820Hz,\ \cdots \tag{11}$$

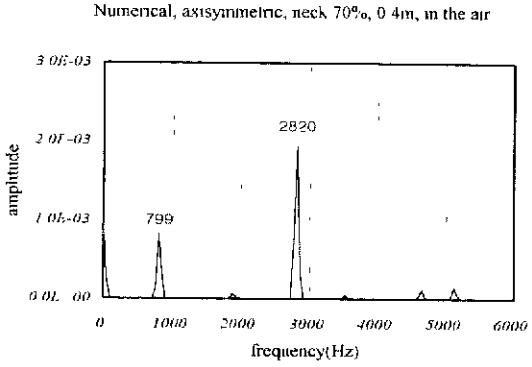

(a) location of neck : 0.4m

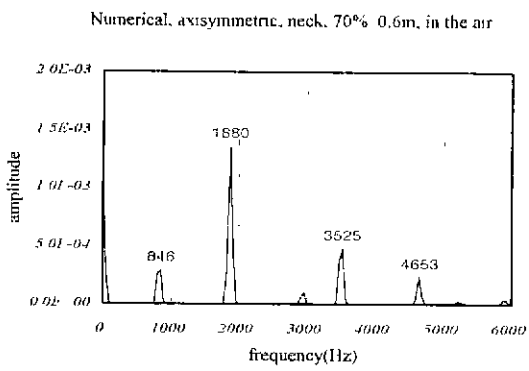

(b) location of neck : 0.6m

Fig. 3 Amplitude spectrums of shafts with necks in the air

This results can be used as a reference guide to check whether the defects occur or not in the shafts.

2.4 Numerical Studies for the Shafts with Neck in the Air

The impact responses were numerically investigated by varying the size and location of defects. Fig. 3 shows the amplitude spectrums of the shafts containing necks at a depth of 0.4m and 0.6m respectively, and the size of the neck is 70% of the cross-sectional area. When the neck is at a depth of 0.4m, the calculated fundamental frequency is 940 Hz, but the first resonance frequency is measured 799 Hz and the second is measured 2820 Hz. The reason that the measured resonance frequency corresponding to the length of shaft is shifted to a lower value is considered to be the fact that the neck reduces the stiffness of the mock-up shaft. This shift toward a lower value is the key to detecting the presence of the flaw. In addition, multiple wave reflections between the impact surface and the surface of the neck produce a large amplitude peak, 2820 Hz in the spectrum at the frequency corresponding to the depth of the neck, and thus make it easy to locate the neck. Using this 2820 Hz, we can estimate the location of the neck to be 0.33m as follows.

$$L = \frac{V_{rod}}{2 \times f} = \frac{1880}{2 \times 2820} = 0.33\,m \qquad (12)$$

This value is smaller than 0.4m, which resulted from the fact that the resonant frequency of defect may be superimposed with the third mode resonance frequency corresponding to the length of shaft.

When the neck is at a depth of 0.6m, the first and the second frequency are measured to be 846 Hz and 1880 Hz, respectively. The fundamental frequency is also shifted to a lower value, and a large amplitude peak, 1880 Hz is produced. Using this 1880 Hz, we can estimate the location of the neck to be 0.5 m approximately. This is also different from the exact location of the neck, and the reason is that the resonance frequency may be superimposed with the second resonance frequency corresponding to the length of shaft as in the previous case.

3. Experimental Studies

3.1 General

Experimental studies were carried out to verify the results obtained from the finite element analyses of shafts in soil as well as in the air, and to investigate the factors influencing the impact-echo results. The impact-echo testing system consists of an impact source and a receiving transducer. In this studies on shafts, several steel balls were used as impact sources, and accelerometer was used as a transducer. Waveforms were recorded and analyzed using a dynamic signal analyzer.

The monocast cylindrical mock-up shafts, 0.1 m in diameter and 1.0 m long, were used to study the impact-echo test. The rod wave speed in the solid shaft

was determined to be 1880 m/sec by the free-free resonance column test (Kweon, 1998). In contrast to concrete material, the monocast material has advantages that it is homogeneous, and the intentional defects can be easily made at desired depths and sizes. In this study, the defects include axisymmetric voids, non-axisymmetric voids, and necks of which the size by area varies 30%, 40%, 50%, 60%, 70%, and 80%, and bulbs of which the size varies 200% and 400%. The location of the defects was set to be at the depth of (a) 0.4m, and (b) 0.6m to minimize the superposition effect of the frequencies corresponding to the defect and the whole length of the shaft. The experimental program is summarized in Table 1, and the shapes of defects in the mock-up shafts are shown in Fig. 4 and Photo 1.

To simulate the monocast mock-up shaft in the air and to

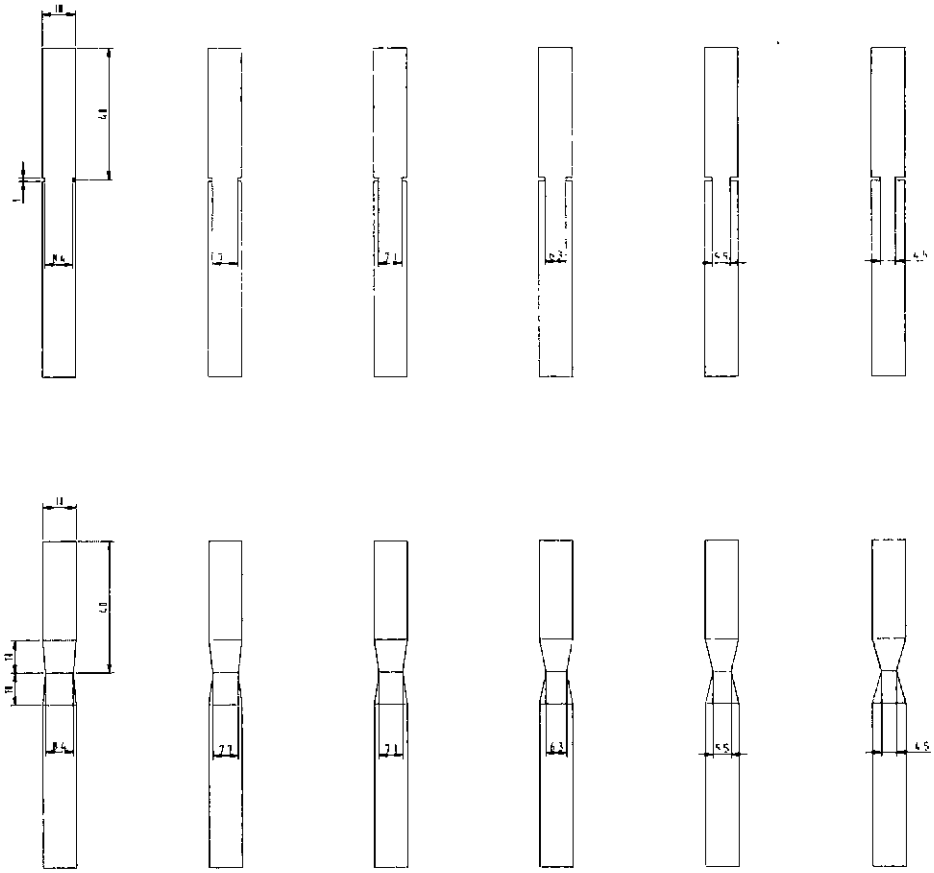

(a) Axisymmetic voids and necks

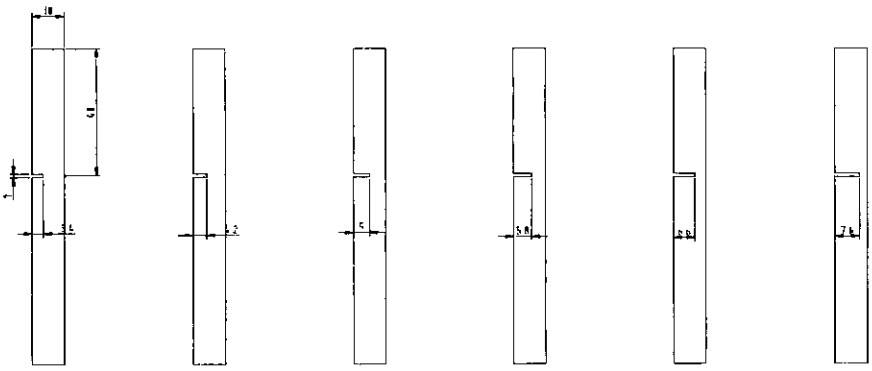

(b) Non-axisymmetric voids

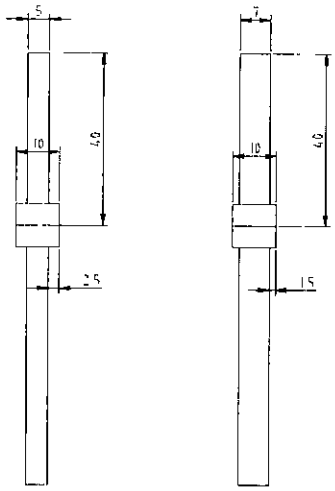

(c) Bulbs

Fig. 4 Shape and Geometry of the defective mock-up shafts

satisfy the free-free end condition, the mock-up shafts were put upon the styro-foam that is soft and light material with minimal acoustic impedance. Subsequently, impact -echo tests were also carried out for the shafts embedded in soil.

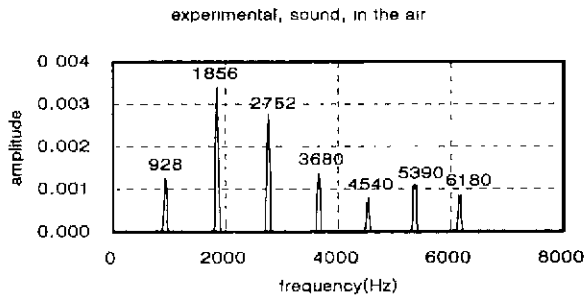

Fig. 5 Amplitude spectrum of solid shaft in the air

3.2 Shafts in the Air

3.2.1 Solid Shaft

The amplitude spectrum of the solid shaft in the air is shown in Fig 5, where the resonance peaks are 928 Hz, 1856 Hz, and 2752 Hz. As shown by the finite element analysis, this pattern of peaks at the depth frequency and its multiples is a characteristic of a solid shaft in the air.

The results of the experiment on solid shafts are in good agreement with the results obtained numerically, giving

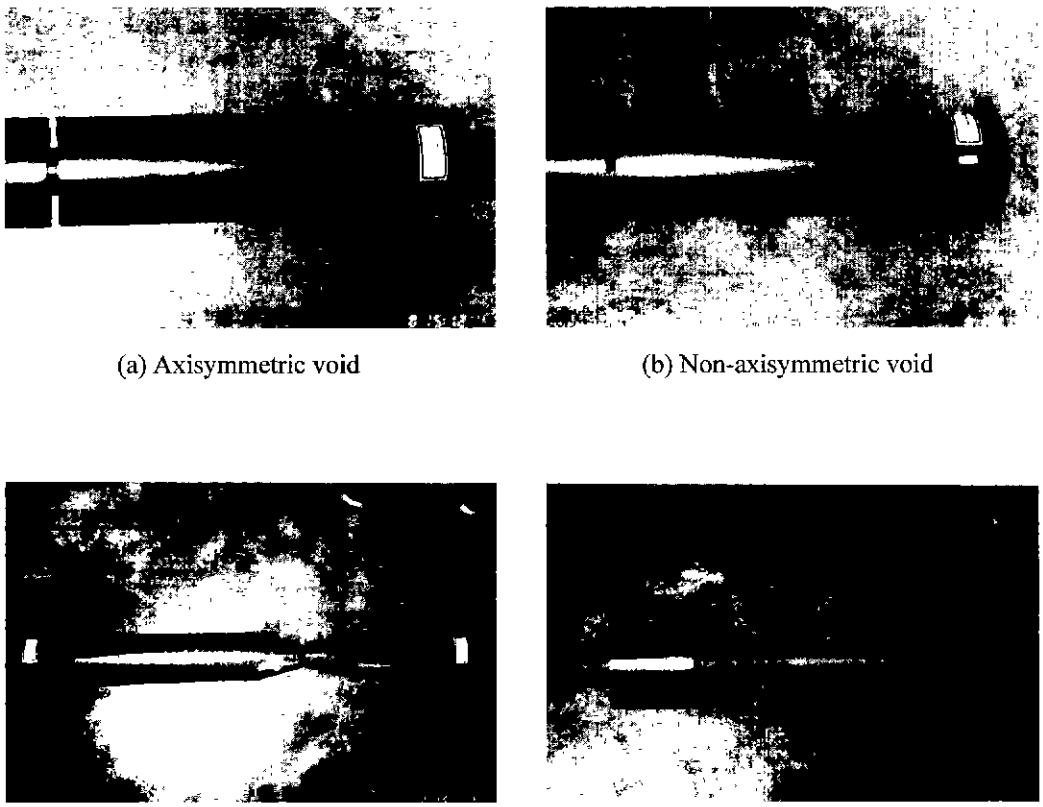

(a) Axisymmetric void

(b) Non-axisymmetric void

(c) Neck

(d) Bulb

Photo 1. Shape of the defective mock-up shafts

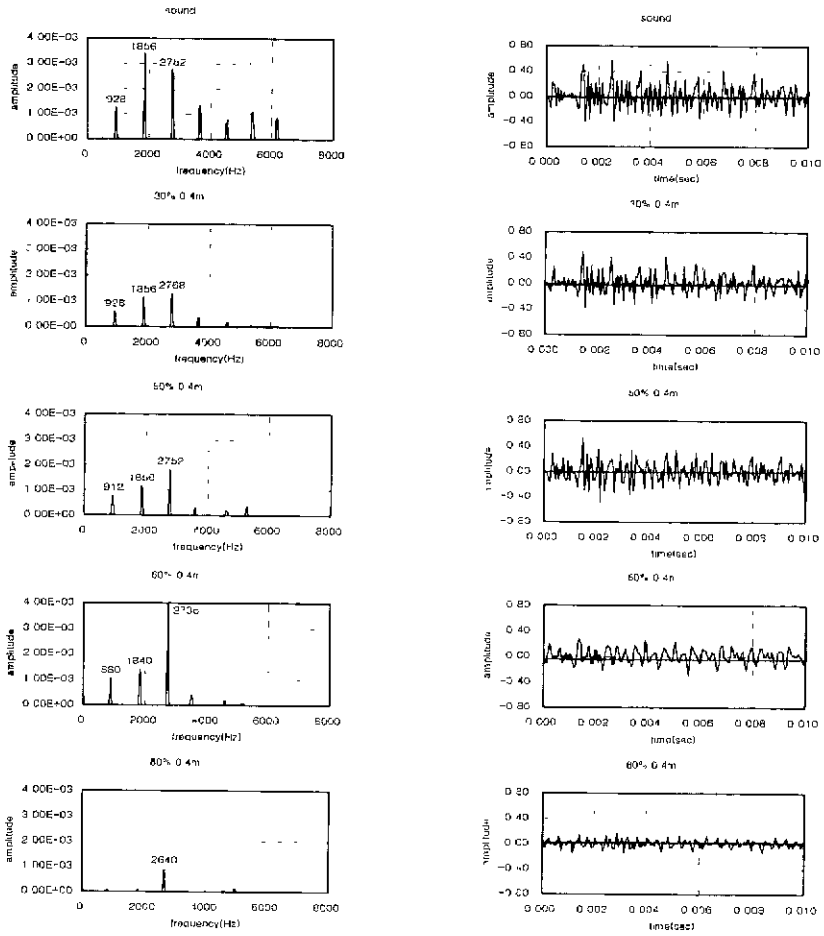

(a) frequency domain (b) time domain

Fig. 6 Impact responses of shafts containing axisymmetric voids in the air

confidence in the reliability of the finite element models.

3.2.2 Axisymmetric Voids

Fig. 6 shows the amplitude spectrums and acceleration-time traces for the shafts containing axisymmetric voids at a depth of 0.4m under the top surface of mock-up shaft determined by the impact-echo test. Test results of various void sizes (sound, 30%, 50%, 60%, 80%) are plotted together for the comparison purpose. The presence of void can be identified by the amplitude spectrum and the location of the void can be also

Table 1. Summary of experimental parameter

condition	type of defect	size of defect(%)	location of defect (m)
in the air	neck	30,40,50,60,70,80	0.4, 0 6
	axisymmetric void	30,40,50,60,70,80	0.4, 0 6
	non-axisymmetric void	30,40,50,60,70,80	0.4, 0 6
	bulb	200,400	0.4, 0 6
in soil	neck	30,40,50,60,70,80	0.4, 0 6
	axisymmetric void	30,40,50,60,70,80	0.4, 0 6
	non-axisymmetric void	30.40,50,60,70,80	0.4, 0.6
	bulb	200,400	0.4, 0.6

determined approximately if the area reduction exceeds more than 60%, where the resonance corresponding to void is dominant. However, the exact location of the voids cannot be obtained even when the area reduction is up to 80%. In this case, the resonance frequency corresponding to the void is considered to be 2640 Hz, and the location of the void can be calculated as 1880/2/2640 = 0.36m. This difference can be explained by the superimpose of the resonance frequency of void with the third mode of resonance frequency of the shaft length. It is shown that the void is located at a depth of 0.4m and the third mode of resonance corresponds to the length of 0.33m. For a reliable interpretation of the impact-echo test, therefore, the possibility of the superimposition should be considered in the analyses.

3.2.3 Necks

Fig. 7 shows the impact responses of mock-up shafts containing necks of which the size vary 30%, 50%, 60%, 70%, and 80% at 0.4m under the top of the surface of the mock-up shaft. The presence of necks can be identified in the amplitude spectrum if the area reduction is more than 50%. Test results show that the greater the area reduction becomes, the clearer the void resonance frequency in the amplitude spectrum becomes. This fact can be also explained by the time trace of acceleration in Fig. 6(b). The waveform of the shaft containing 30% area reduction neck consists of more than two distinguishable sine waves, but as the area reduction becomes greater, the waveform almost consists of single sine waveform. This is because the void resonance frequency is superimposed by the third resonance frequency corresponding to the length as discussed before. As a result, the resonance frequency of this superimposed signal is dominant in the amplitude spectrum.

3.3 Shafts in Soil

In order to investigate the impact responses more specifically, the experimental parametric studies were carried out for the mock-up shafts embedded in soil as well as in the air. When a propagating wave in a monocast mock-up shaft is incident upon the interface between the shaft and the soil, some of the energy is reflected and some is transmitted into the soil. The amount of reflected energy depends on the relative acoustic impedances of shaft and soil. Less difference in the acoustic impedance allows more energy to be transmitted into the soil. Accordingly, the surface displacement response obtained from a shaft in soft soil would be larger than that obtained from a shaft in dense soil because less energy is lost to the surrounding soil.

The mock-up shafts were embedded in the container filled with loose sands. To obtain satisfactory results in soil model, it is important for the wave propagating into soil not to be reflected back to the model. Therefore, the container with larger diameter is desired. In this study, the container with a diameter of 1.0m, and a height of 1.2m was used, and the effect of reflected wave from the container boundary was negligible.

3.3.1 Axisymmetric Voids

Fig. 8 shows the impact responses of mock-up shafts containing axisymmetric voids of which the size vary 30%, 50%, 60%, and 80% at 0.4m under the top of the surface of the mock-up shaft. As seen in Fig. 8(b), the reflected signals from the bottom and/or the defect can be clearly noticed compared with signals in the air, and this is because the higher frequency signals may be filtered out during the propagation of waves into the soil. In addition, it is interesting to note that the waveform of the sound shaft is quite different from that of the shaft containing axisymmetric voids, and the defects such as axisymmetric voids can be identified clearly in the time domain, even when the size of voids is 30%, whereas it is difficult to detect the same size of voids confidently in amplitude spectrum. Also, the voids become greater, the higher amplitude spectrums are obtained, and this is because the waveform of the solid shaft is mixed with reflected waves on the interface of voids, and consequently is apt to be consisted of single sine wave.

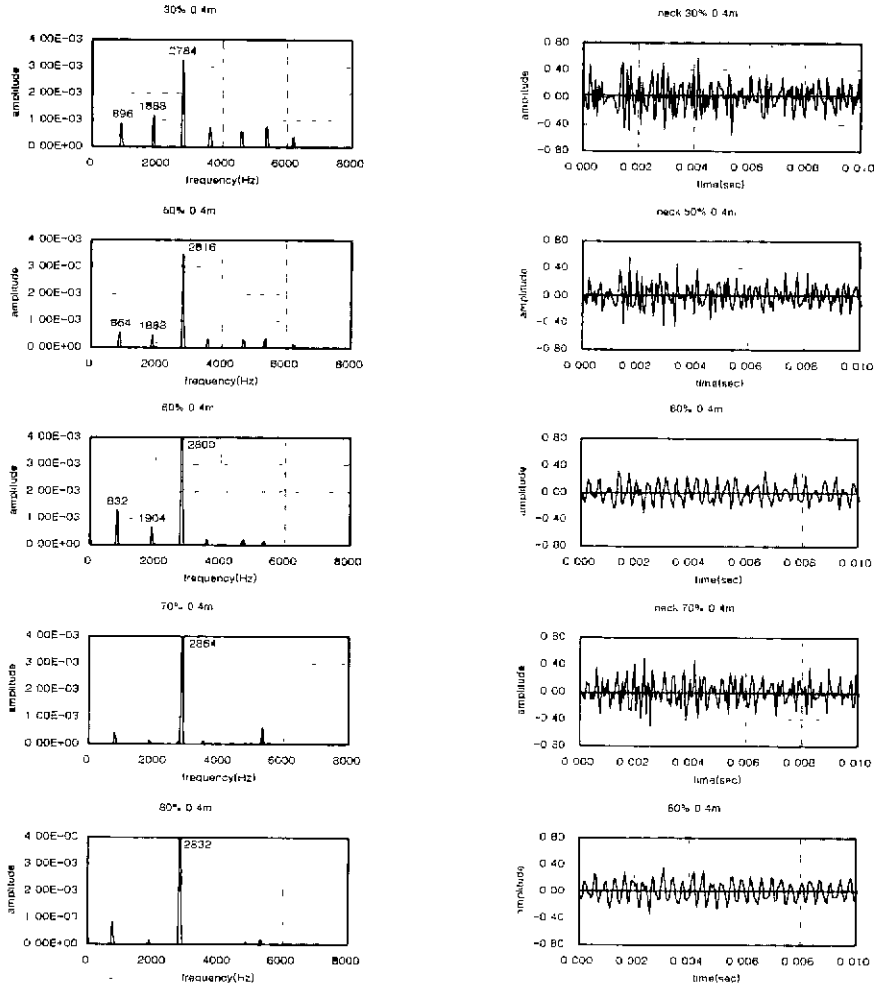

(a) frequency domain (b) time domain

Fig. 7. Impact responses of shafts containing necks in the air

It is shown that the presence of the flaw can be identified by amplitude spectrum if the size of void is greater than 50%, and the location of the voids is estimated to be 0.34m.

3.3.2 Non-axisymmetric Voids

Fig. 9 shows the impact responses of mock-up shafts containing non-axisymmetric voids of which the size vary 30%, 40%, 50%, 60%, and 70% at 0.6m under the top of the surface of the mock-up shaft. The impact responses obtained here are similar to those of the axisymmetric voids, and it is noticeable that the flaws can be detected in time domain even when the size of the void is only 30%, whereas in frequency domain, the flaws cannot be identified with confidence.

3.3.3 Bulbs

In this study, two types of bulbs were tested ; the bulbs increase the cross-sectional area of the shaft by 200% and 400% respectively. The response of a shaft containing a bulb is different from the neck. A bulb acts to increase the stiffness of a cross-section, rather than to decrease its stiffness as is the case for a void or neck. The effectively stiffer bulb section behaves as though it has a higher acoustic impedance. Therefore, the compressive rod wave incident upon this section reflect as a compressive wave. Thus the first arrival of the rod wave reflected from the bulb cross-section will cause an upward signal rather than

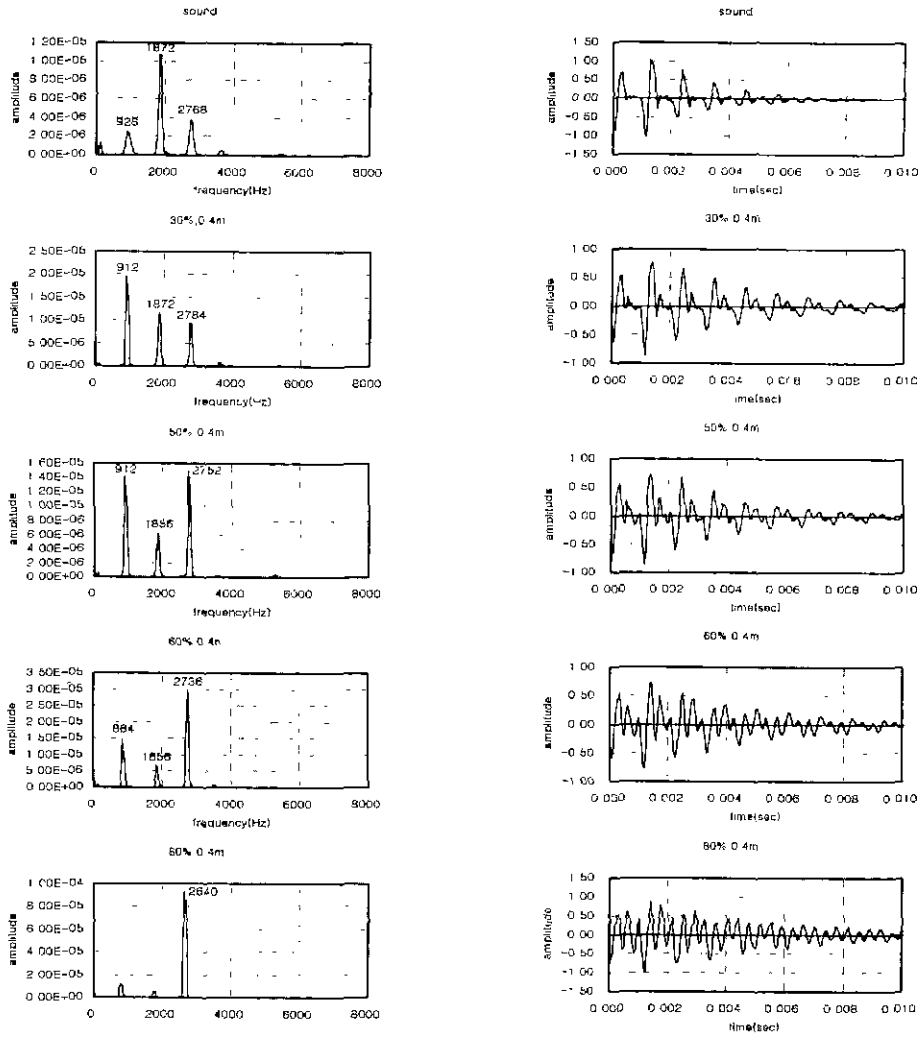

(a) frequency domain (b) time domain

Fig. 8 Impact responses of shafts containing axisymmetric voids in soil

a downward signal, as has been observed for the previous flaw cases. This fact can be identified clearly in the time domain as shown in Fig. 10(b) and (c) (notice the arrow in the figure).

Also, the fact that the bulb section behaves as though it has a higher acoustic impedance can be explained from the ratio of 960 to 2624 is 1 : 2.75 which gives the ratio of 1 resonance peak frequencies, 960 Hz and 2624 Hz. The: 3 approximately as in the case of free-fixed boundary condition,

$$f_n = \frac{n\ V_{rod}}{4T},\ \mathrm{n} = 1,\ 3,\ 5,\ \cdots \qquad (13)$$

The presence of bulb can be identified in waveform, and the location of it can be also estimated approximately by the equation (13). However since the integer 4 in equation (13) is observed to be variable according to impedance difference, therefore it is difficult to locate the bulb exactly.

4. Correlation between the Size and Estimated Location of Defects

It is obtained from the experimental studies that the estimated location of the defects by the impact-echo method is closer to the exact value, according as the defect size becomes greater as shown in Fig. 11. In addition, it is observed that the non-axisymmetric voids can be easily

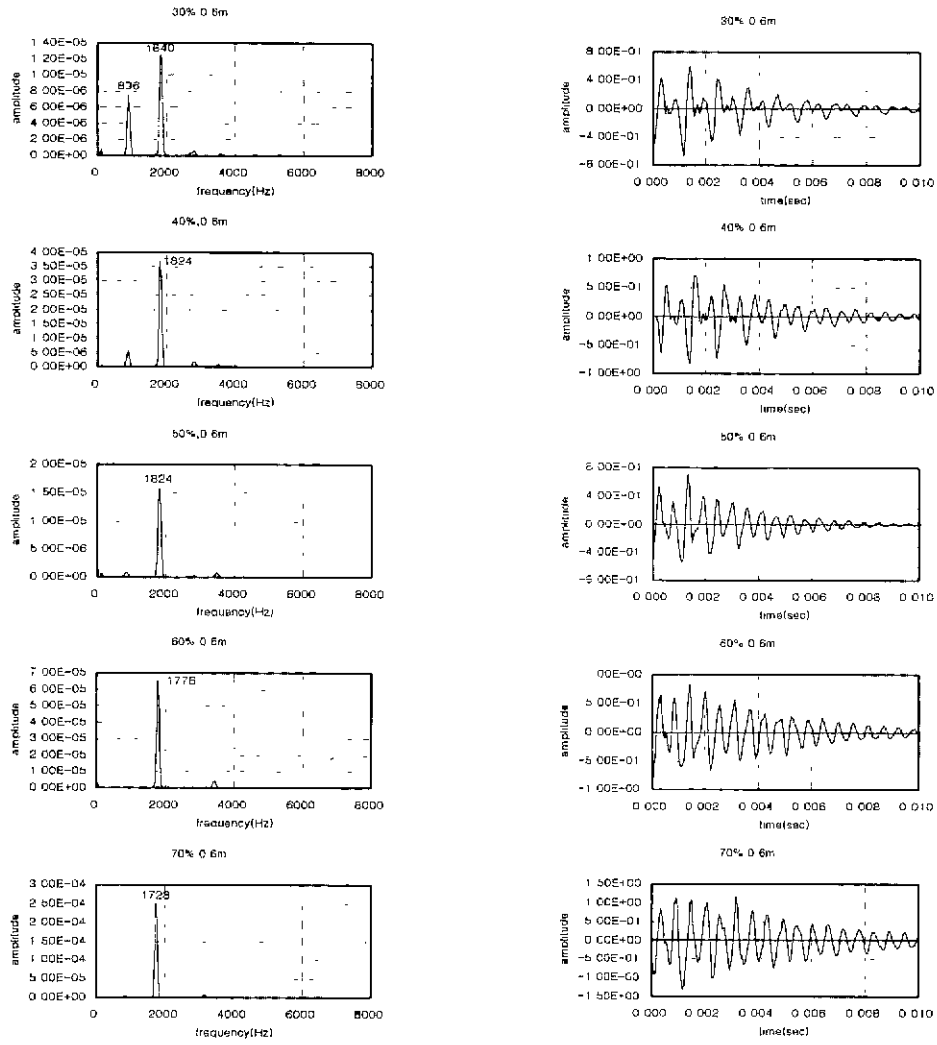

(a) Frequency domain (b) Time domain

Fig. 9 Impact responses of shafts containing non-axisymmetric voids in soil

detected than axisymmetric voids.

On the other hand, this figure shows the limitations that the exact location of defect cannot be predicted by the impact-echo method, even when the defect size exceeds more than 80% of the cross-sectional area of the shaft. This is because the resonance frequencies corresponding to the defects are superimposed by the second and/or third resonance frequencies corresponding to the whole length of the shaft. However, since the actual drilled shafts constructed in construction site are long, these limitations will be able to be recovered with minimal difficulties.

5. Conclusions

The objectives of the studies presented in this paper are to understand the impact responses by extensive numerical and experimental parametric studies, and thus to establish the basis for the use of the impact-echo method in practice. Then, the conclusions obtained are as follows :

1) The results of the experimental studies on mock-up shafts are in good agreement with the results obtained numerically.
2) When a defect is present in the shaft, the existence of it can be identified in both amplitude spectrum and waveform. A shift of the fundamental frequency toward a lower value is the key to detecting the presence of the defect. In addition, multiple wave reflections between the impact surface and the surface of the flaw produce a large amplitude peak in the spectrum at the frequency corresponding to the depth of the defect.

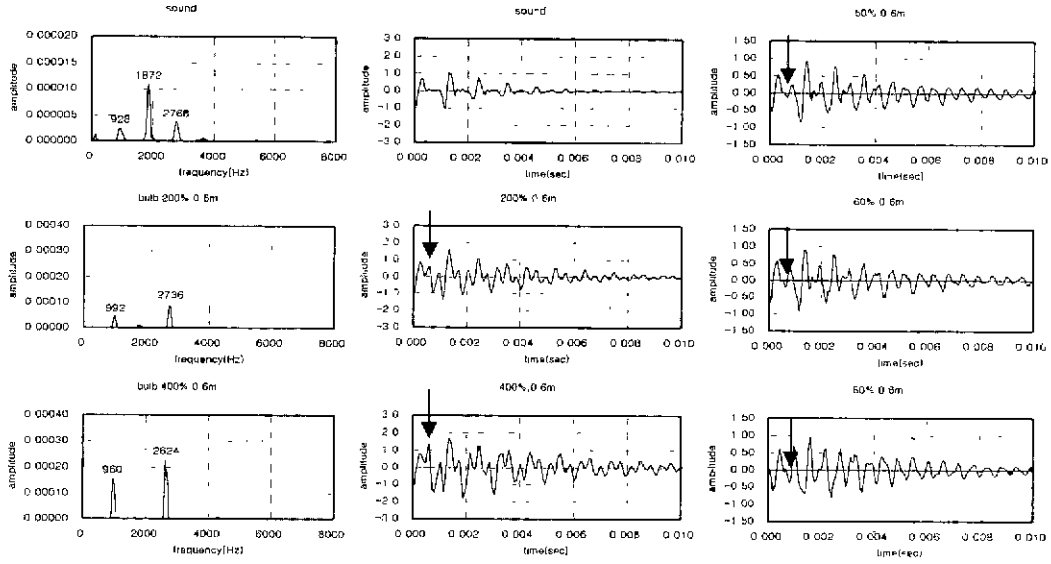

(a) frequency domain (bulbs) (b) time domain (bulbs) (c) frequency domain (voids)

Fig. 10. Comparisons of impact responses for shafts containing bulbs and axisymmetric voids

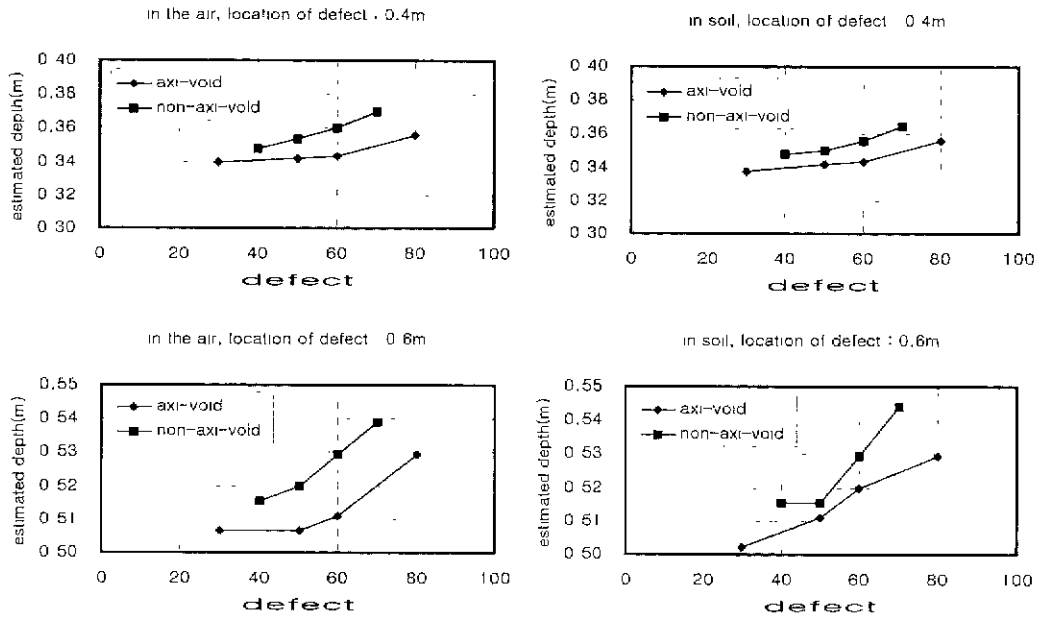

(a) shafts in the air (b) shafts embedded in soil

Fig. 11 Correlation between the size and estimated location of defects

3) The defects such as axisymmetric voids, non-axisy mmetric voids, and necks can be located in amplitude spectrum, if the area reduction is more than 50%, whereas the defects can be identified in the time domain, if the area reduction is more than 30%, which could provide the enhanced data interpretation methodologies of impact-echo test. Also it was observed that the non-axisysmmetric voids were able to be more easily detected than axisysmmetric voids.

4) A bulb in a shaft can be detected, and distinguished from other types of voids by using the waveform to identify the upward signals and by observing the first

and second resonance frequency interval of 1 : 3, which caused by reflections from the enlarged cross section.

Acknowledgements

This work was partially supported by the Korea Science and Engineering Foundation (KOSEF, 98-0601-0201-3). The authors express their appreciation for this support.

References

1. Abramson, H.N., Plass, H.J., and Ripperger, E.A. (1958), "Stress wave propagation in rods and beams", Advances in Applied Mechanics, Vol. 5, 111.
2. Hsiao, C., Lin, Y., and Chang, C. (1999), "Nondestructive evaluation of concrete quality and integrity in composite columns", NDT&E International, Vol. 32, pp.375-382.
3 Kim, D.S., Park, Y.H. (1999), "Impact Echo Responses of Deep Foundations", Proc. of the 1st International Conference on Advances in Structural Engineering and Mechanics, Choi. C.K., Schnobrich, W.C. eds, Seoul, Korea, pp.1399-1404.
4. Kweon, G.C. (1998), "Alternative MR Testing Methods for Subgrade and Subbase Materials Considering Deformational Characteristics of Soils", Ph. D Dissertation, Korea Advanced Institute of Science and Technology, pp.34-40.
5. Liao, S. (1994), "NONDESTRUCTIVE TESTING OF PILES", Ph. D Dissertation, The University of Texas at Austin, pp.9-205.
6. Lin, Y., Sansalone, M., and Carino, N.J. (1991), "Impact-Echo Response of Concrete Shaft", Geotechnical Testing Journal, Vol. 14, No. 2, pp.121-137.
7. Sansalone, M., and Streett, W.B. (1997), Impact-Echo Nondestructive Evaluation of Concrete and Masonry, BULLBRIER PRESS, ITHACA, N.Y., pp.29-320
8. Park, Y.H. (1998), "Integrity Evaluation of Deep Foundations Using Impact Echo Method", MS Thesis, Korea Advanced Institute of Science and Technology, pp 20-69.
9. Timoshenko S.P., and Goodier J.N (1970), Theory of Elasticity, 3rd ed., McGraw-Hill. Inc.

(received on May., 19, 2000)